Hindawi
International Journal of RF and Microwave Computer-Aided Engineering
Volume 2024, Article ID 6660144, 20 pages
https://doi.org/10.1155/2024/6660144

Review Article

A Review of Over-the-Air Testing Methods for Performance Measurement of Antennas and Devices in Communication Systems

Siqi Duan,[1] **Weimin Wang**,[1] **Bihua Tang**,[1] **Yongle Wu**,[2] **and Yuanan Liu**[1]

[1]*School of Electronic Engineering, Box 282, Beijing Key Laboratory of Work Safety Intelligent Monitoring, Beijing University of Posts and Telecommunications, Beijing, China*
[2]*School of Integrated Circuits, Beijing University of Posts and Telecommunications, Beijing 100876, China*

Correspondence should be addressed to Weimin Wang; wangwm@bupt.edu.cn

Received 7 July 2023; Revised 8 December 2023; Accepted 27 December 2023; Published 16 January 2024

Academic Editor: Yen-Sheng Chen

With the fast development of communication techniques, over-the-air testing has developed into the main testing method for current communication systems due to its advantages including no cable connection, high measurement efficiency, and independence from environment. OTA testing has become almost the only solution for 5G system testing especially after the popularity of 5G massive multiple-input-multiple-output. In this paper, we summarize the three main methods of OTA testing including the reverberation chamber-based method, the radiation two-step method, and the multiprobe anechoic chamber- (MPAC-) based method, among which we focus on the MPAC method systematically. In the MPAC method, there are two main channel synthesis techniques that have been heavily studied, namely, prefaded signal synthesis and plane wave synthesis. We summarize the current main research based on these two techniques including probe configurations, probe selection algorithms, and probe design based on the PFS technique and the design of plane wave generators based on PWS technique. The main comparisons are made for the performance of different probe selection algorithms and the performance of different plane wave generators as well as the latest advances.

1. Introduction

As the name implies, over-the-air (OTA) testing is a developing and interesting testing method which transmits signal employing radiation between antennas instead of cable connection. During early days, OTA testing is primarily applied to 2G and 3G communication systems for the measurements of single-input-single-output (SISO) including total radiation power and total isotropic sensitivity. However, with the continuous development of communication technologies, critical techniques including orthogonal frequency division multiplexing and multi-input-multi-output (MIMO) are introduced into 4G systems making SISO no longer functional due to its dissatisfaction on high throughput.

There exist three kinds of OTA testing approaches for 4G systems including reverberation chamber- (RC-) based method, radiated two-stage (RTS) method, and multiprobe anechoic chamber- (MPAC-) based method, the latter two of which are on the basis of anechoic chambers. These three methods are authorized by 3GPP for measuring radiation performance of UEs' multiantennas and MIMO receivers in High Speed Packet Access and Long-Term Evolution devices [1].

For the sake of improving capacity and spectrum utilization, 5G systems further develop MIMO techniques by manufacturing antennas into miniaturized integrated devices with massive units. If traditional testing methods are still adopted to 5G systems, a great number of cables are demanded which greatly increases the error rate, complexity, and cost of test equipment [2]. On the contrary, OTA testing possesses superiorities of repeatability, reliability, and high measurement efficiency [3] making it leading method of 5G and emerging systems. There are mainly two kinds of testing patterns in 5G OTA testing including

performance testing and radio frequency testing. The principal assignment of performance testing is to precisely reestablish the objective wireless channels under measurement area.

MPAC is supposed to be the most promising method of reconstructing channel features through flexibly changing channel scenarios by software including controllable angle of arrival (AOA) and angle spread (AS) [4]. 2-D MPAC with 16 probes and RTS are employing to test at FR1 which are also the testing methods of LTE adopting different number of probes. 3-D MPAC is adopted to test at FR2 due to the requirements of wavelength and area of test zone.

In this paper, a detailed and systematic summary on the above three OTA testing methods will be conducted among which MPAC is highlighted. Current research on MPAC testing method is mainly focused on probe weight allocation algorithms suitable for MPAC. A certain number of probes are attached to output ports of the channel emulator to restore real channel environment in MPAC which is the main cost source of testing. How to select a certain number probes from massive candidates to conduct testing without harming testing accuracy is the current research hotspot. A large number of probe selection algorithms have been proposed, and this paper conducts a summary on probe selection algorithms in recent years.

One of the most important configuration parameters for OTA testing is the design of test probes. Horns and Vivaldi antennas are usually employed as the test probes in current OTA testing. However, multireflection between these probes will affect the ripple level of quiet zone (QZ) resulting in performance deterioration of testing systems including the ability of small signals' detection, RF parameter measurements, and MIMO throughput [5, 6]. A significant method to reduce ripple level of QZ is to enhance the absorption capacity of the anechoic chamber among which the design of testing probes is an important aspect. This paper summarizes main design schemes of testing probes for OTA testing in recent years, predicts the mainstream development direction on future design of OTA testing probes, and clarifies the main challenges currently faced with.

Besides, far field range is adopted to directly test the radiation pattern of antenna under test (AUT) which means AUT is placed at the far field of testing probes. The testing distance of direct far field becomes extremely large owing to large size and high working frequency of 5G antennas. There mainly exist two approaches under research to reduce testing distance including compact antenna test range (CATR) and PWGs, and this paper will report on these two methods, respectively.

The authors in [7] briefly reviewed the standardization progress and corresponding testing methods of 5G MIMO OTA performance testing. This article focused on discussing the comparison between 4G and 5G testing methods specified in the standards. However, the progress of the reverberation chamber-based method and radiated two-stage method is not discussed, and the introduction of the MPAC method was not detailed enough. Kong et al. [8] presented new midfield developments including the gray box approach and a midfield prototype system covering both frequency ranges one and two to address challenges in 5G massive MIMO base station OTA RF test. However, a comparison between OTA testing methods is missed.

The authors in [9] discussed the testing schemes of 5G millimeter wave devices and analyzed their applicability and limitations in OTA performance evaluation of 5G millimeter wave user devices. However, this article did not compare the advantages and disadvantages of testing schemes at different testing distances. Researchers in [10] not only reviewed the MIMO OTA testing methods and the latest standardization progress in 3GPP but also discussed the work plan of 3GPP and the potential challenges of 5G MIMO OTA testing. This article provided a detailed comparison of the testing parameters for the three frequency bands but did not delve into the testing methods for the 5G frequency band.

Jing et al. [11] discussed the latest progress in radiated two-stage MIMO OTA testing methods. As an auxiliary method for 5G MIMO OTA testing, this article did not discuss the advantages and disadvantages of this method. Table 1 shows the specific comparison between the above papers and this paper.

The structure of this paper is organized as follows. Section 2 introduces related progress of reverberation chamber-based method of OTA testing. Section 3 introduces related progress of radiated two-stage method of OTA testing. Section 4 introduces related progress of anechoic chamber-based method of OTA testing. The comparison between the three methods and the challenges and the future development are summarized in Section 5. Finally, the contributions and conclusions are drawn in Sections 6 and 7, respectively.

2. Reverberation Chamber-Based Method

As shown in Figure 1, RC is consisted of a mode stirrer and several antennas. RC-based method was mainly applied for EMC measurements to obtain strong radiation fields with small input power and has a development history over 20 years before being applied to communication performance testing [13]. From 2000, RCs have been developed into a powerful tool for communication performance measurement to conduct measurements on radiation performance of compact antennas and other active mobile terminals due to its advantages including low cost and no need for moving the device under test (DUT).

2.1. Antenna Efficiency Measurement. RC-based method is usually adopted in testing nondirectional indicators of wireless equipment such as antenna efficiency which is calculated in

$$\eta = \frac{R_R}{R_R + R_L}, \tag{1}$$

where R_R and R_L are the radiation impedance and the antenna loss impedance, respectively.

In early days, several RC-based methods for testing antenna efficiency were proposed [14–19]. However, these

Table 1: A comparison between other review papers and this paper.

Methods	Classification criteria	Including three methods	Including comparisons	Discussing probe configurations	Summarizing probe selection algorithms
[7]	Frequency	No	No	Yes, two kinds	No
[8]	Testing distance	No	No	No	No
[9]	Testing distance	No	No	No	No
[10]	Frequency	No	Yes	Yes, three kinds	No
[11]	/	Only RTS	Yes	No	No
This paper	Probe configuration	Yes	Yes	Yes, in detail	Yes, in detail

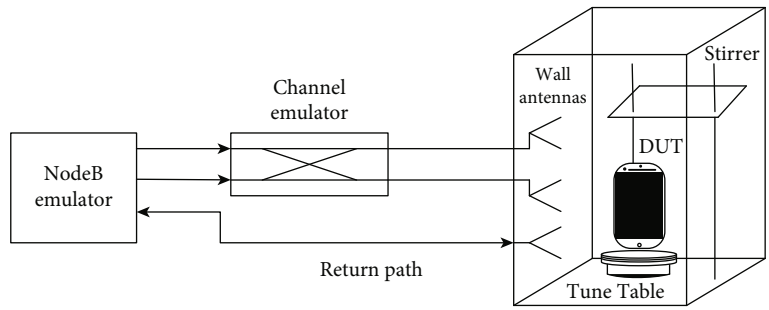

Figure 1: Configuration reverberation chamber for 2×2 MIMO OTA testing in [1].

methods suffer from a common drawback that one of the following requirements must be met:

(1) An antenna with known efficiency is adopted as reference

(2) The two antennas used in the measurements have the same radiation characteristics

This poses significant limitations to the widespread application of RC-based method. To overcome these limitations, many other methods have also been proposed. An extensively applicate method for measuring antenna efficiency without the requirement of reference antennas was proposed by Wheeler [20]. However, this method depended on a continuous conductive surface named "Wheeler Cap" and requires a new conducting sphere when testing a new frequency. Therefore, this method is limited for antenna efficiency measurements of electric small-sized antennas.

Azremi et al. [21] validated through experimental measurements for the first time that RCs could be applied in testing multipath performance of antennas especially radiation efficiency, and the results showed high comparability with traditional Wheeler Cap-based method. Different from Wheeler Cap, a RC-based method for electric big-sized antennas without the requirement of reference antennas was proposed by Lee et al. [22] to measure antenna efficiency which overcame the limitations of Wheeler Cap and could be applied in wide frequency band. Further, Holloway et al. [23] proposed three methods to test total efficiency of unknown antennas including single-antenna-, double-antenna-, and triple-antenna-based methods which overcame the drawbacks of above methods. However, these three methods share a common prerequisite that the loss of AUT should be much smaller compared with the loss of RC resulting the inability in efficiency measurements of antennas with low efficiency. Besides, an improved two-antenna-based method was proposed by Xu et al. to obtain antenna efficiency in RCs which combined the traditional reference antenna-based method and the single-antenna-based method [24]. This method broke restrictions generated by methods with necessary requirements of reference antennas through introducing a virtual antenna and could be applied in measuring antennas with arbitrary loss providing possibility of measuring antennas with low efficiency in RCs.

2.2. Radiation Pattern Measurement. However, testing radiation patterns of antennas through RCs is of great difficulty due to the existence of multipath interference which can be hardly achieved by data processing through complicate algorithms. There are three methods to test radiation patterns of antennas in RCs including K-factor-based method, Doppler frequency-based method, and correlation coefficient-based method.

2.2.1. K-Factor-Based Method. Fiumara et al. [25] reconstructed radiation pattern of antennas in free space through field measurements in RCs for the first time. Further, a significant conclusion was confirmed by Lemoine et al. [26] that measurements of antennas' directivity in RCs could be accurately realized through precise estimation of K-factor on which a new method based on the Rician factor was proposed to reconstruct radiation pattern of radiation device in RCs. On the basis of [20], Fiumara et al. further explored the performance of method proposed in [27] in actual environment and indicated that the performance in actual

environment was degraded compared with that in ideal environment, namely, full reverb.

2.2.2. Doppler Frequency-Based Method. García-Fernández et al. [28] proposed a method to test radiation pattern of antennas based on plane wave decomposition through which antennas' directivity was measured in RCs for the first time. However, this method has a disadvantage that N transmitting antennas located on AUT's line of sight are required and connected to the fixed AUT which contributed greatly in cost increasing. For the purpose of saving measurement time and improve efficiency, García-Fernández et al. [29] carried out only one measurement for each angle under research to test radiation pattern of antennas which obtained the same accuracy through much less time.

2.2.3. Correlation Coefficient-Based Method. Xu et al. [30] proposed a testing method of antennas' radiation pattern in RCs based on spherical wave decomposition which represented the advantages of practicality, economy, and high efficiency. However, this correlation coefficient-based method was unable to be applied in RCs with load. To address this problem, Zheng et al. [31] achieved improvement on traditional technique and adopted a compensation method through reference antenna to realize the reconfiguration of radiation pattern of AUT in RCs with load. However, the stirring effect of antennas cannot be ignored in the implementation of the above method which results in error occurrence when applied in small RCs. Corresponding solution is to utilize the method in large RCs which shows superiority compared with traditional method.

Different from the method adopted in [28, 30], Puls et al. [32] simplified the objective problem through averaging scattering parameter data of uncorrelated propeller position which showed the same testing results with that obtained in anechoic chamber by antenna manufacturers. The results in [32] represent the advantages of RC-based method of simplicity and economy when applied in measurements of antennas' directivity.

3. Radiated Two-Stage Method

Fundamental configuration of RTS method is shown in Figure 2. The basic procedures of RTS method are to measure MIMO radiation pattern of DUT first, and after that, the convolution between the radiation pattern of DUT and the selected MIMO OTA channel model is conducted. OTA testing methods based on RCs achieve reducing cost which could only simulate limited characteristics of channel models. However, accurate modeling of 3-D multipath can be achieved through RTS method with only one SISO anechoic chamber which improves testing flexibility together with much lower cost.

Traditional two-stage method represents an obvious disadvantage that self-interference of the DUT is neglected in throughput testing due to the cable connection with DUT. To address this problem, Yu et al. [34] proposed RTS method which tests throughput through OTA radiation overcoming drawbacks of traditional two-stage method together with retaining its advantages whose channel models represent high flexibility and accuracy. An analysis was conducted by Jing et al. [35] to discriminate the applicability of RTS in 4Rx MIMO OTA testing and 5G NR FR1 radiation performance testing on which a significant conclusion was obtained that RTS method showed scalability from 2Rx to 4Rx on UE MIMO OTA testing at sub-6 GHz. Besides, RTS method can be also applied in radiation performance testing in multichannel. With the development of communication techniques, RTS method is the unified method for conducting OTA testing at FR1 according to applicable standards and two dual-polarized probes located at different positions are required to perform 4×4 MIMO OTA testing as shown in Figure 2.

However, current report on uncertainty analysis is extremely limited which shows great importance on evaluating the accuracy of testing results and developing error elimination methods. To solve this problem, a mathematical model was established by Shen et al. [36] regarding the reporting error in testing system which introduced error factors. An uncertainty analysis was conducted on the basis of the above model on MIMO throughput measurements obtained through RTS method. Report error in radiation pattern measurements of UEs was evaporated from testing throughput signals' generation and downlink power computation which enhanced accuracy and consistency of RTS and contributes to further research on 5G OTA testing.

4. Multiprobe Anechoic Chamber-Based Method

OTA testing becomes preferred alternative of 5G MIMO testing and future emerging systems due to its ability of reproducing real channel scenarios in limited environment of the laboratory avoiding the need of modification and connection on DUT. Key issue of MIMO OTA performance testing lies in reconstructing spatial characteristics of real channel models on which MPAC configuration is proposed. The main challenges of MPAC-based method lie in the high complexity of the measurement configuration and the high cost of the testing system which is mainly produced by the high cost of multiport channel emulators. MPAC-based method is adopted as the reference method of FR OTA testing in which 2-D MPAC system employing 16 dual-polarized probes equally spaced is applied in OTA testing at FR1 as shown in Figure 3. On the contrast, 3-D MPAC-based method with 6 dual-polarized probes is adopted as the standard method for OTA testing at FR2 as shown in Figure 4 [1].

According to field range of spatial sampling area, OTA testing systems for antenna performance testing in anechoic chambers can be classified into three types including reactive near field, radiated near field, and far field. Among them, near-field method adopts measurements in radiation near-field range of DUT and then obtains the radiation pattern by adopting near-field to far-field transform algorithms which requires the smallest range of measurement area. However, sampling of amplitude and phase on the surface surrounding the DUT is demanded among which phase sampling is of great difficulty in practical operation. In addition, coupling between probes and DUT is almost unable to

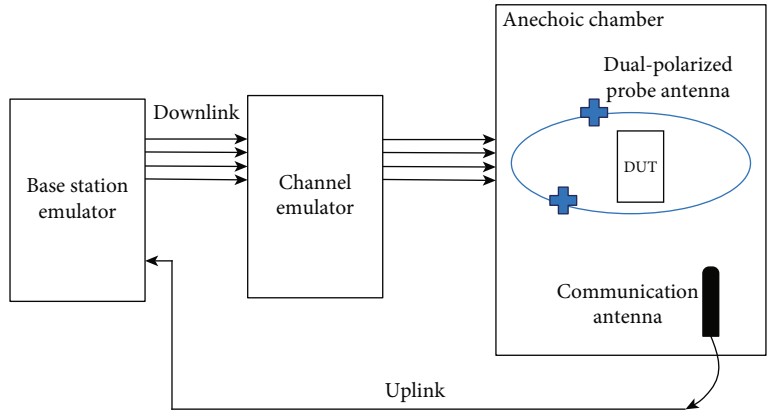

Figure 2: Fundamental configuration of RTS system [33] for MIMO OTA testing at FR1.

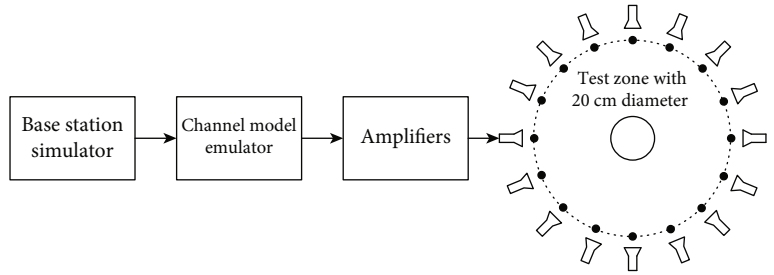

Figure 3: Fundamental configuration of MPAC system [33] for MIMO OTA testing at FR1.

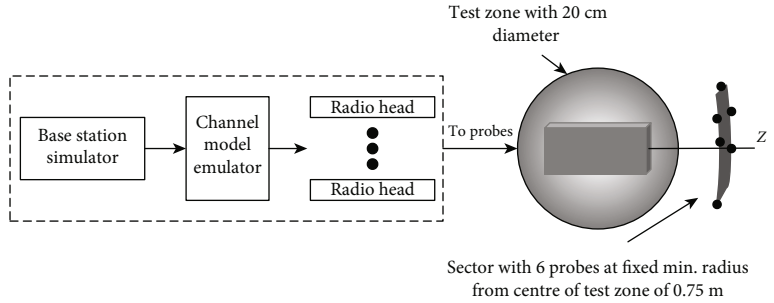

Figure 4: MPAC system configuration [33] for MIMO OTA testing at FR2.

compensate because the sampling distance is far too close. Based on the above problem, Kyösti et al. [4] proposed two kinds of channel simulation technologies including prefaded signal synthesis (PFS) and plane wave synthesis (PWS) among which PFS is widely applied in OTA testing. PWS and PFS are both able to simulate arbitrary target channel model, and the main distinction between them lies in that probes in PFS are real-weighted yet probes in PWS are complex-weighted. Therefore, PWS is relatively more complex due to its requirements of both power calibration and phase calibration. On the contrary, PFS requires only phase calibration.

Each probe in anechoic chamber is directly connected to output ports of the channel emulator to imitate real communication channels, and the expensive channel emulators are the main cost sources of MIMO OTA testing. Adopting an increase in the number of sampling probes can enhance the testing accuracy, yet the testing cost is greatly improved simultaneously. Compromise between testing accuracy and testing cost is the main problem that industry and academic circle are concerned about currently. The simulation accuracy of spatial correlation depends on the distribution of probes [37]. In early days, contribution on channel simulation technologies is mainly focused on fixed probe configuration and the goal is to seek out the optimal weight of each probe. However, both the weight and the location are required to be optimized in practical test. Therefore, the main research direction and challenge are to reconstruct real channels at high accuracy with fewer probes. Currently, there are three categories of probe selection algorithms including iterative algorithms, spatial angle mapping algorithms, and heuristic algorithms. A systematic exposition on probe selection algorithms will be conducted according to different MPAC configurations in this section.

4.1. Spatial Correlation. Channel spatial correlation is adopted as the indicator to estimate the accuracy of the simulated channel model in PFS. A position pair composed of two isotropic probes m and n is employed to describe features of the two sampling points where the probes are placed [36]. The space correlation of the objective channel model is calculated in

$$\rho = \oint \exp\left(jk\left(\vec{r}_m - \vec{r}_n\right)\cdot\vec{\Omega}\right)P(\Omega)d\Omega, \tag{2}$$

where k is the wave number, $\vec{r}_m$ and $\vec{r}_n$ are position vectors of sampling probes m and n, $\vec{\Omega}$ is the unit vector of the solid angle Ω, and $P(\Omega)$ is the spherical power spectrum which satisfies the equation $\oint P(\Omega)d\Omega = 1$. The space correlation of the simulated model is calculated in

$$\widehat{\rho} = \sum_{l=1}^{L} w_l \exp\left(jk\left(\vec{r}_i - \vec{r}_j\right)\cdot\Phi_l\right). \tag{3}$$

Minimum sum reconstruction error is taken as the objective function in most of the current research which is calculated in

$$\min_{w} \|\widehat{\rho}(\mathbf{w}) - \rho\|_2^2, \tag{4}$$

where $\mathbf{w} = [w_1,\cdots,w_L]$ is the power vector composed of power weights of all probes which satisfies the equation $0 \le w_l \le 1$. Therefore, the root mean square error (RMSE) of the simulated channel accuracy is calculated in

$$\mathrm{RMSE} = \sqrt{\frac{1}{N_0}\sum_{n}^{N_0}|\rho(m) - \widehat{\rho}(m)|^2}, \tag{5}$$

where N_0 is the number of sampling location pairs and $\rho(m)$ and $\widehat{\rho}(m)$ are target space correlation and simulated space correlation of the mth position pair, respectively. Besides, maximum error is adopted by researchers to evaluate the simulated accuracy.

Channel models and probe configurations mentioned in this paper are shown in Tables 2 and 3, respectively.

4.2. Probe Selection Algorithms

4.2.1. 2-D MPAC Configuration. The setup of MPAC OTA testing was first described by Kyösti et al. including a fading emulator, an anechoic chamber, and a set number of sampling probes [38] as shown in Figure 5. Probes are uniformly distributed on a horizontal plane around the DUT in 2-D MPAC configuration. Testing signals are generated by a BS simulator and then fed to a multichannel fading emulator. A multipath environment is created by the channel emulator including path delay, Doppler propagation, and fast fading.

In 2-D MPAC configuration, clarifying the number of probes has great significance due to the fact that the testing cost is proportional to the number of probes. The distance between probes was analyzed by Imai et al. according to spatial correlation of received signals obtaining a certain number of probes [39]. A MIMO OTA system with 4, 8, and 16 probes around the measurement area was studied by Laitinen et al. [40] on the basis of which a conclusion was obtained that the number of probes in a MPAC testing could be calculated in equation (2).

$$K = 2\left[\frac{\pi D}{\lambda}\right] + 1, \tag{6}$$

where the square bracket indicates rounding the number in the bracket to its nearest integer and D is the diameter of the measurement area in Figure 5.

Two algorithms were proposed to determine the weight and angle position of each probe under flexible configuration including genetic algorithm (GA) and multishot algorithm [41]. Channel models adopted in [41] included single-cluster channel model (C1), SCME Umi TDL channel model (C18), and SCME Uma TDL channel model (C19) [1] as shown in Table 2. Three probes were selected to realize a measurement area of 1λ for C1 with the maximum spatial correlation error of 0.14 and 0.3 through GA and multishot, respectively. Eight probes were selected to realize a measurement area of 1.5λ for C18 with the maximum spatial correlation error of 0.12 by multishot which showed better performance than GA. On the contrary, 8 probes were selected to realize a measurement area of 1.5λ for C19 with the maximum spatial correlation error of 0.25 by GA which showed better performance than multishot.

Selective distribution probe algorithm (SDPA) was proposed by Fan et al. and validated through a MPAC system in Academy of Broadcasting Planning [42]. Four probes were selected to realize a measurement area of 0.7λ by SDPA which showed the same accuracy compared with 8-probe configuration indicating that half resource of probes was saved.

A flexible probe configuration based on particle swarm optimization was proposed by Wang et al. to decrease the number of probes which accurately reconstructed the spatial correlation of the base station [43]. Four probes were selected to reconstruct the space correlation with the maximum spatial correlation error of 0.029 when the DUT is an antenna array of 8×8. Besides, 8 probes were selected to reconstruct the space correlation with the maximum spatial correlation error of 0.03 when the DUT is an antenna array of 16×16.

Two probe selection algorithms were proposed by Fan et al. based on 2-D sectorized MPAC configuration for base station testing including discrete particle swarm optimization (DPSO) and multiple iteration algorithm [42]. 2-D sectorized configuration P1 and channel model C18 were selected to evaluate the effect of the above two algorithms. The channel model was the same with that in [41], and a comparison between them is conducted in Table 4.

Previous sectorized MPAC configuration was mostly combined with spatial channel model extensions to carry out probe selection which was not suitable for 5G OTA

Table 2: Channel models adopted in referenced articles.

Channel model	PAS	PES	Comment	Paper no.
C1	AoA = 22.5° AS = 35°	/	Single Laplacian-shaped spatial cluster	40
C2	AoA = 0° ASA = 35°	EoA = 0° ESA = 10°	Single Laplacian-shaped spatial cluster	48, 50, 53, 60
C3	AoA = 15° ASA = 35°	EoA = 15° ESA = 10°	Single Gaussian-shaped spatial cluster	48, 50, 53
C4	Uniform	EoA = 0° ESA = 10°	Uniform-shaped PAS and Laplacian-shaped PES	48, 52
C5	AoA = 2.7° ASA = 3°	ZoA = 106.9° ZSA = 3°	Single Gaussian-shaped spatial cluster	51
C6	AoA = 22.4° ASA = 10°	ZoA = 112.9° ZSA = 8°		
C7	AoA = 3.2° ASA = 15°	ZoA = 105.2° ZSA = 7°		
C8	AoA = −5.5° ASA = 20°	ZoA = 78.33° ZSA = 8°		
C9	AoA = 22.0° ASA = 24°	ZoA = 84.6° ZSA = 10°		
C10	AoA = 26.5° ASA = 30°	ZoA = 107.4° ZSA = 15°		
C11	AoA = 15° ASA = 35°	EoA = 0° ESA = 10°	Single Laplacian-shaped spatial cluster	52
C12	AoA = −3.2° ASA = 2°	ZoA = 96.2° ZSA = 3°		
C13	AoA = −30° ASA = 11°	ZoA = 73.4° ZSA = 7°	Single Gaussian-shaped spatial cluster	59
C14	AoA = 26.4° ASA = 15°	ZoA = 109.1° ZSA = 8°		
C15	AoA = 37.8° ASA = 20°	ZoA = 115.4° ZSA = 10°		
C16	AoA = 9.7° ASA = 25°	ZoA = 93.4° ZSA = 15°		
C17	AoA = −10.7° ASA = 30°	ZoA = 87.5° ZSA = 15°		
C18	SCME Umi TDL			
C19	SCME Uma TDL			
C20	Multicluster channel model proposed in [12]			48
C21	Multicluster channel model proposed in [4]			52

testing. A 2-D MPAC sectorized configuration with 16 probes uniformly distributed was proposed by Yu et al. for the first time to validate the practicality of sectorized configuration in sub-6 GHz OTA testing [12]. Besides, an intelligent cuckoo search algorithm was introduced to optimize the probe selection process which selected 4, 6, and 3 probes for channel models CDL-A, CDL-C, and CDL-D from total number 14, 14, and 19 probes, respectively, under the condition that the maximum RMS < 0.1.

Similarly, Yang et al. came up with a probe selection algorithm based on standard beam filtering characteristics [44] and validated it through 5G channel models as [12] took. Under the same condition of RMSE < 0.1, the algorithm adopted in [44] selected 14 probes from total 16 probes which decreased the total cost by 1/8. A comparison between the methods adopted in [12, 44] is shown in Table 5 since they chose the same channel models to evaluate the performance. The difference lies in that the researcher in [44] took two different scenarios to evaluate the performance of the algorithm.

4.2.2. 3-D MPAC Configuration. The main advantage of massive MIMO is the antenna array with controllable beam which demands accurate 3-D characterization of channel

Table 3: Probe configurations of the referenced articles.

Case	Probe configuration	Paper no.
P1	Boresight direction = 0°, azimuth angle ∈ [−60°, 60°] $N = 24$ probes uniformly distributed	42
P2	$\theta = -90°\ 90°, \varphi = 0$ $\theta = -45°\ 45°, \varphi = 23\ 74°\ 125°\ 177°\ 228°\ 280°\ 331°$ $\theta = 0°, \varphi = 0°\ 45°\ 90°\ 135°\ 180°\ 225°\ 270°\ 315°$	46
P3	$\theta_1 = -30°, \phi_{1i} = -90° + i \cdot 90°, i \in [1, 4]$ $\theta_2 = 0°, \phi_{2i} = -45° + i \cdot 45°, i \in [1, 8]$ $\theta_1 = 30°, \phi_{3i} = -67.5° + i \cdot 90°, i \in [1, 4]$	
P4	$\theta_1 = 30°, \phi_{1j} = -180° + i \cdot 30°, i \in [1, 12]$ $\theta_2 = -30°, \phi_{2j} = -180° + i \cdot 15°, i \in [1, 24]$ $\theta_3 = -30°, \phi_{3j} = -180° + i \cdot 30°, i \in [1, 12]$	48
P5	$\theta_1 = 45°, \phi_{1j} = -180° + i \cdot 45°, i \in [1, 8]$ $\theta_2 = 10°, \phi_{1j} = -180° + i \cdot 22.5°, i \in [1, 16]$ $\theta_3 = -10°, \phi_{1j} = -180° + i \cdot 22.5°, i \in [1, 16]$ $\theta_1 = -45°, \phi_{1j} = -180° + i \cdot 45°, i \in [1, 8]$	48, 53
P6	$\theta_1 = 18°, \phi_{1j} = -180° + i \cdot 30°, i \in [1, 12]$ $\theta_2 = -30°, \phi_{2j} = -180° + i \cdot 15°, i \in [1, 24]$ $\theta_3 = -18°, \phi_{3j} = -180° + i \cdot 30°, i \in [1, 12]$	52
P7	$\theta_1 = 30°, \phi_{1j} = -180° + i \cdot 45°, i \in [1, 8]$ $\theta_2 = 0°, \phi_{1j} = -180° + i \cdot 11.25°, i \in [1, 32]$ $\theta_3 = -30°, \phi_{3j} = -180° + i \cdot 45°, i \in [1, 8]$	53
P8	$\theta_1 = 30°, \phi_{1j} = -180° + i \cdot 90°, i \in [0, 3]$ $\theta_2 = 0°, \phi_{2j} = -180° + i \cdot 11.25°, i \in [0, 31]$ $\theta_3 = -30°, \phi_{3j} = -180° + i \cdot 90°, i \in [0, 3]$	60
P9	$\theta_1 = 45°, \phi_{1j} = -180° + i \cdot 45°, i \in [0, 7]$ $\theta_2 = 0°, \phi_{2j} = -180° + i \cdot 22.5°, i \in [0, 15]$	
P10	Coverage of vertical direction: 60° Coverage of horizontal direction: 120° Interval between adjacent probes: 10°	51, 59
P11	Coverage of vertical direction: 60° Coverage of horizontal direction: 120° Spacing between adjacent probes: 5°	
P12	Coverage of vertical direction: [−21°, 21°] Coverage of horizontal direction: [−60°, 60°] Interval between adjacent rows: 3° Interval between adjacent columns: 6°	57
P13	Coverage of vertical direction: [−30°, 30°] Coverage of horizontal direction: [−90°, 90°] Interval between adjacent probes: 5°	60

model especially the power azimuth spectrum (PAS) for the beamforming [62]. High testing accuracy is obtained through increasing the number of the probes in MPAC OTA testing which will greatly improve the testing cost in 3-D MPAC configuration as shown in Figure 6. Therefore, how to pick out a certain number of probes from massive available probes to perform testing with high accuracy at low cost is the most concerning problem currently.

There are two indicators to perform evaluation of probe configuration [46] including related precision measurement and comprehensive error which represent the same results of the diameter of the measurement area and can be applied to evaluate the effect of probe configuration under arbitrary channel model and measurement area diameter.

Fan et al. proposed three algorithms under arbitrary probe configuration for PFS and PWS including brute force algorithm (BFA), multishot algorithm, and successive probe cancellation (SPC) algorithm [47] which relied on the convex optimization framework proposed in [48]. Two probe configurations including P4 and P5 and a channel emulator with 16 output ports were adopted to estimate the performance of the above three algorithms which realized a measurement area of 1λ. The channel emulator with 16 output ports meant that 16 probes would be selected from total 48 probes to reconstruct the channel model. The computation will become enormous when BFA is adopted to select probes from a large number of probes since BFA traverses all possible probe combinations to find the optimal one which makes the error of space correlation smallest. Several probes with smallest contribution will be deleted in each shot when multishot algorithm is adopted to select probes which reduces overall computation compared with BFA. On the contrast, probes with the greatest contribution will be selected by successive interference cancellation technique which is widely applied in wireless communication when SPC is adopted to select probes. A comparison between methods adopted in [41, 47, 49] is conducted in Table 6 since these methods adopted either same channel models or same probe configurations to evaluate the performance.

A flexible 3-D probe configuration method based on genetic algorithm (GA) was proposed by Gao et al. in which the location of each probe was flexible [49]. Two channel models including C2 and C3 were adopted to validate the performance of the method which selected 7 probes from total 16 probes to reconstruct the space correlation of the channel model. The results showed better performance compared with 3-D fixed probe configurations in [50–52].

Two probe selection algorithms were proposed by Yang et al. including decremental selection algorithm (DSA) and selection algorithm based on alternating search (SAAS) which chose 10 and 9 probes for the chosen channel models, respectively. Besides, the performance of SAAS was better than that of DSA for the three chosen channel models.

In response to the problems of traditional algorithms in [47] including time-consuming and insufficient accuracy, a memetic algorithm- (MA-) based probe selection approach was proposed by Wang et al. which selected fewer probes with higher accuracy [53]. Two channel models including C2 and C3 and four probe configurations including P2, P3, P5, and P7 were adopted to validate the performance of the above MA-based method. A performance comparison between the methods in [53, 54] is made in Table 7. However, the method should be further applied into 5G channel models and future channel models possessing more complex characteristics which will greatly improve the application of MPAC-based OTA testing method.

A new MPAC testing system based on switch matrix and a fast selection algorithm for 3-D probe configuration was constructed by Guo et al. [55] which implemented multiplexing of different MIMO OTA testing systems including

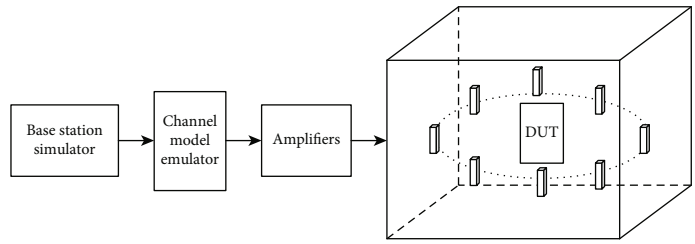

Figure 5: 2-D MPAC test setup of OTA testing in [38].

Table 4: Comparisons between algorithms in [41, 42].

No.	Channel model	Algorithm	Probe setup	$\lvert\widehat{\rho}-\rho\rvert$	Cluster number					
					1	2	3	4	5	6
40	C18	GA	8 probes flexible	MAX	0.17	0.20	0.65	0.24	0.21	0.18
				RMS	0.05	0.06	0.35	0.07	0.06	0.05
		Multishot		MAX	0.16	0.09	0.44	0.09	0.10	0.15
				RMS	0.07	0.05	0.25	0.05	0.05	0.07
42	C18	DPSO	8 probes P1	MAX	0.22	0.30	0.07	0.20	0.22	0.10
				RMS	0.18	0.25	0.05	0.17	0.17	0.07
		Multi-iteration		MAX	0.23	0.12	0.32	0.20	0.22	0.08
				RMS	0.19	0.09	0.26	0.16	0.19	0.07

Table 5: A comparison between algorithms evaluated with 5G channel models.

No.	Scenario	Number of probes under different channel models				
		CLD-A	CLD-B	CLD-C	CLD-D	CLD-E
43	/	4	/	6	3	/
44	UMa	12	14	12	8	8
	UMi	8	10	8	6	6

2-D, 3-D, 3-D simplified, and 2-unit MPAC systems. This composite system satisfies requirements of multifunctional MIMO OTA testing which save at most 3/4 port resource with high accuracy.

4.2.3. 3-D Sectorized MPAC Configuration. Lengths of 5G BSs are about 1 m resulting in the distance of far field exceeding 30 m which cannot be directly tested in anechoic chamber. At the same time, massive MIMO techniques are adopted in BSs of 5G systems to enhance spectral efficiency and coverage resulting in the requirement of enormous channel emulators in OTA testing which poses huge challenges to the performance testing of BSs due to its high cost. To address the above problem, Kyösti et al. proposed a 3-D sectorized MPAC system as shown in Figure 7 [58] in which the distances between each probe and the center of the measurement area are the same. The space of the anechoic is fully utilized which contributes a lot to reduce the cost of OTA testing.

A disadvantage of multishot algorithm is that recalculation of power weights is repeatedly conducted through convex optimization after the probe set candidate is renewed resulting in abundant of useless calculations. For the purpose of improving the efficiency of calculation, a method based on neural network was proposed by Li et al. to obtain the angle location and weight of probes which adopted regularization technique realizing optimization through only one training process [59]. Two probe configurations including P10 and P11 and three kinds of channel models were employed to estimate the performance of the method as shown in Table 8. It is worth mentioning that neural network was introduced to OTA testing for the first time in this paper which greatly improved the calculating efficiency and overcame the drawback of multishot algorithm in [47]. Similarly, artificial bee colony algorithm (ABCA) was introduced into MPAC OTA testing for probe selection by Zhang et al. [60] which performed better performance compared with multishot algorithm in [47]. Different from other algorithms, this paper conducted link level simulation to evaluate the downlink throughput of two CDL channel models.

A probe selection algorithm named forward allocation based on orthogonal matching pursuit (OMP) was proposed by Wang et al. to conduct OTA testing for 5G massive MIMO BSs [61]. It is worth mentioning that an equipment rotation scheme was proposed to coordinate with the algorithm which represented better performance compared with other algorithms for BSs. Similarly, OMP was also adopted by Sun et al. to obtain the location and the power weight of probes on the basis of compressed sensing theory [45]. Six single-cluster channel models and three multicluster channel models with two probe configurations were employed to evaluate the performance of the algorithm as shown in Table 6 which showed better performance compared with multishot algorithm.

In response to the problems including sensitivity to initialization and instability of results of traditional heuristic

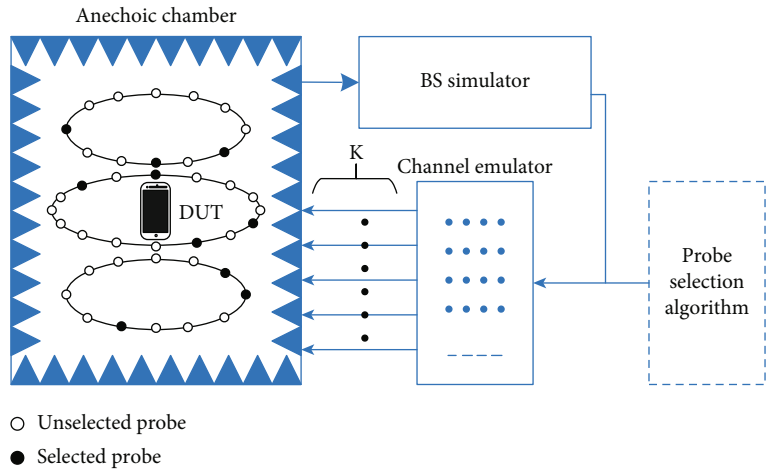

Figure 6: 3-D MPAC OTA testing setup in [45].

Table 6: Comparisons between algorithms in [39, 47, 49].

No.	Channel model	Algorithm	Probe setup	$\lvert\widehat{\rho}-\rho\rvert$	
40	C1	GA Multishot	3 probes flexible	MAX	0.15 0.3
50	C2	GA	7 probes flexible	MAX RMS	0.0377 0.0165
	C3			MAX RMS	0.0335 0.0127
48	C2	One shot	P4	MAX	0.031
			P5		0.06
		Multishot	P4		0.03
			P5		0.057
		SPC	P4		0.031
			P5		0.06
	C3	One shot	P4		0.281
			P5		0.16
		Multishot	P4		0.28
			P5		0.16
		SPC	P4		0.281
			P5		0.16
	C4	One shot	P4		0.029
			P5		0.061
		Multishot	P4		0.029
			P5		0.036
		SPC	P4		0.029
			P5		0.061
	C20	One shot	P4		0.024
			P5		0.023
		Multishot	P4		0.023
			P5		0.02
		SPC	P4		0.024
			P5		0.023

algorithms including GA [41], PSO [43], ABC [60], and MA [53], a probe selection algorithm based on differential evolution (DE) was proposed by Wang et al. [56] to reconstruct the characteristics of channel models with high accuracy. Three probe configurations including P8, P9, and P13 and two channel models were adopted to estimate the performance of the proposed algorithm. A comparison between the method in [45] and other methods is made in Table 6 since they all adopted RMSE as the indicator to evaluate the effectiveness of the methods.

However, 3-D configuration is not recommended as the testing scheme at the beginning of MPAC OTA testing due to its high complexity [62]. Therefore, 3-D configuration MPAC OTA testing is a significant direction of research and possessing great prospects. In this section, common probe configurations including 2-D, 3-D, and 3-D sectorized with corresponding probe selection algorithms under various channel models are summarized. Next, probe design for MPAC OTA testing in recent years will be introduced.

4.2.4. Characterization of Probes in Chambers. The number and configuration of probes are important testing parameters in the anechoic chamber-based OTA testing method which create a significant impact on measurement accuracy and efficiency. In addition, massive MIMO antenna arrays have been widely adopted in OTA testing including PWGs and reflectarrays which both contain a number of antenna elements. Each array element in the above probes contains specific information which will produce a corresponding and nonnegligible impact on the final performance. Therefore, it is of great significance to accurately characterize each array element and evaluate the information contained in each element to identify malfunctioned elements in ensuring the accuracy of the total information to be conveyed. In recent years, multisine signal waveforms have been widely used for this nonlinear characterization, and the multisine method has been proposed in [63].

The waveform signal of multisine is defined as equation (7) in this method as follows [64]. One option is to provide different sine waves for each antenna array unit, and the entire integrated waveform will present as a complete

Table 7: A comparison of results in [45, 53, 54, 56].

No.	Algorithm	Channel model	Probe setup	Number of probes	RMSE
52	DSA	C4	P6	10	0.05
		C11			
		C21			
	SAAS	C4		9	
		C11			
		C21			
53	MA	C2	P5	9	0.0189
			P7	7	0.0352
			P3	16	0.0434
			P2	24	0.0408
		C3	P5	7	0.1296
			P7	8	0.0848
			P3	16	0.1817
			P2	24	0.1094
59	OMP	C12	P10	8	0.0023
		C13			0.0642
		C14			0.0864
		C15			0.1091
		C16			0.1279
		C17			0.1431
		CDL-A in [57]	P11	16	0.0009
		CDL-B in [57]			0.0189
		CDL-C in [57]			0.0069
60	DE	C2	P8	16	0.0225
			P9		0.0483
			P13		0.0214
		CLD-B in [57]	P8		0.2159
			P9		0.2300
			P13		0.2254

multisine. However, an obvious drawback arises in this case. The beamforming network will in turn excite each antenna unit with different signal waveforms resulting in affecting the beamforming ability of the array.

$$x(t) = \sum_i A_i \cos(\omega_i t + \theta_i). \quad (7)$$

To overcome this limitation, an alternative is to adopt a multisine signal with a common frequency for each array unit and then apply a tick tone with different frequencies to each element on the basis of common frequency. The equation of this method is shown in the following equation [63]:

$$x(t) = \sum_i A_i \cos((\omega_0 + \Delta\omega_i)t + \theta_i), \quad (8)$$

where ω_0 is the common frequency also known as main tone and $\Delta\omega_i$ is tickle tone. The authors in [63] demonstrated the specific implementation of the scheme of feeding multisine signals to each antenna array element to detect malfunctioned ones. Furthermore, Jordão et al. [65] validated the characterization of traditional array antennas adopting the multisine method, demonstrating its effectiveness in characterizing antenna arrays.

The traditional multisine method is usually adopted to characterize array antennas to identify malfunctioned elements in the array which is seen as "forward identification." Inspired by this, Jordão et al. [66] adopted the multisine method to perform beamforming calibration of array antennas. The main tone of all elements operates at the common frequency while the tick tone of each element operates at different frequencies to obtain phase information. Five different MIMO antennas were adopted to verify the effectiveness of the multi-sine-based calibration method.

4.3. Traditional Probe Design for OTA Testing. Probes play a key role in MPAC OTA testing for the reason that its ripple in quiet zone will cause testing error which can be solved through improving probes' absorption. Designs and configurations are the most concerning problems in MPAC OTA testing. Since probe configuration was discussed in detail in the last section, we will focus on the design of probes in this section. Horns and Vivaldi antennas are the most commonly used probes for OTA testing.

Quadruple-ridged horn (QRH) antennas are the traditional schemes for OTA testing due to its excellent performance including wide frequency band and dual polarization. An inverted QRH was proposed for OTA testing with high isolation and low reflection coefficient [67]. It is worth mentioning that it realized one-decade bandwidth with balanced feeding for the first time in recent years. A phased array which adopted horns as elements was proposed by Zhang et al. which showed good performance including high efficiency [62].

Two major parameters of MPAC configuration are the number of sampling probes and the distance between the probes and DUT since they determine the measurement cost of OTA testing [7]. Probes with small sizes are necessary requirements in 5G OTA near-field testing for the purpose of improving sampling resolution and reducing coupling between probes [68]. However, dual-polarized QRHs are no more suitable to be applied in 5G OTA testing owing to its disadvantages including large volumes, high cost, and high reflections. On the contrast, tapered slot antennas (TSAs) are causing widespread attention in 5G OTA testing recently due to its outstanding advantages including ultrawideband, symmetrical radiation pattern, moderate gain, low cross-polarization, high plasticity, and easy manufacturing.

A full-wave analysis was conducted on the distribution of electromagnetic fields of antennas with various slots concluding that double-side TSAs represented the best performance including the widest frequency bandwidth and the lowest cross-polarization among the total 6 traditional TSAs [69]. On this basis, a dual-polarized double-side TSA was proposed by the researcher in [70] to be applied in EMC

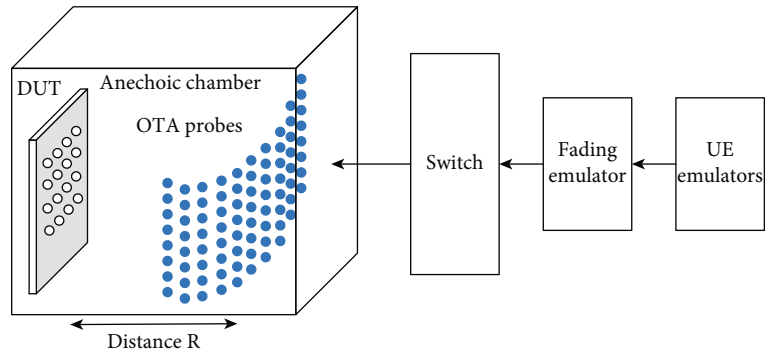

Figure 7: 3-D sectorized configuration [49] for MPAC OTA testing.

Table 8: A comparison of results in [46].

No.	Channel model	Probe setup	Number of probes	RMSD
51	C5	P10	8	0.0227
	C6			0.0795
	C7			0.0642
	C8			0.0455
	C9			0.0810
	C10			0.1084
	CDL-A in [57]	P11	16	0.0347
	CDL-B in [57]			0.0669
	CDL-C in [57]			0.0251

testing which greatly improved the performance of traditional Vivaldi antennas on working bandwidth and the main beam making it become the excellent candidate of OTA testing probes.

However, the realization of excellent performance of Vivaldi antennas at low frequency demands big sizes of antennas [71, 72] which limits its application in 5G OTA testing. Therefore, simultaneously reducing the antenna size and improving the performance at low frequency is the most challenging problem at present.

A wideband dual-polarized Vivaldi antenna was proposed by Sonkki et al. for the purpose of satisfying various wireless standards in MIMO OTA testing systems [73]. However, the results of cross-polarization discrimination were not good enough to a certain extent which could be improved in the future.

A dual-polarized TSA with absorber integrated was proposed by Wu et al. for the application of anechoic chamber OTA testing [74]. The reduction in radar cross section (RCS) was realized through combining the antenna with the absorber which achieved a 10.9 dB reduction on monostable RCS. It is worth mentioning that this is the first design which applied RCS reduction to OTA testing probes providing guidance for the future research work.

Similarly, a dual-polarized probe consisting of two crossed-placed Vivaldi antennas was proposed by Qiao et al. for OTA testing [75]. There are two highlights in the design of this antenna. Firstly, a rotational symmetry radome in 3-D printing was adopted to address the problem of difficult processing due to the low elastic modulus of the dielectric materials. Besides, microwave-absorbing materials with optimized locations were adopted to further reduce the RCS and the size of the antenna.

The designs in [69, 75] are the most representative antennas for OTA testing in recent years. It is found that the compact size and the performance at low frequency are difficult to be balanced combining the performance of these two antennas. Therefore, designing of antennas with compact size, wide bandwidth, low RCS, and excellent performance at low frequency is the challenge OTA testing is facing and the most promising direction of research.

OTA testing plays a significant role in estimating the radiation performance and the link performance of wireless communication systems especially 5G communication systems. However, multiple reflections between probes are the main factors which restrict the enhancement of performance in quiet zone. Probes with low RCS become the most concerning designs to improve the testing performance through suppressing multiple reflections between probes. Traditional methods for reducing RCS can be divided into two types including scattering and absorbing [76], the former includes shaping and metasurfaces, and the latter includes radar absorbing materials and absorptive metasurfaces. However, the performance of probes will be harmed if the above methods are adopted directly to the designing process. Therefore, designing of compact probes with excellent radiation performance and low RCS is the most concerning direction in the future research.

4.4. Emerging Probe Design for OTA Testing. Current research on PFS is mainly focused on the design of plane wave generators (PWGs). As the name implies, far-field range means that the DUT is placed in the far field of the probes where radiation patterns of DUTs can be directly measured. The testing distance becomes very large of direct far field due to the characteristics of 5G antennas including big size and high working frequency. Therefore, two schemes are under research to reduce the testing distance including compact antenna test range (CATR) and plane wave generators. For the first scheme, a reflectarray antenna is located in the CATR system [77–79] to provide a far-field environment in its near field. However, reflectarray antennas become extremely expensive due to the big size of DUT including BSs. For the second scheme, a PWG is a special

kind of antenna array which generates uniform plane wave within its near field. A far-field environment can be generated through allocating proper complex weight to each element of the array. However, current designing of PWGs is mainly theoretical research which has not applied into practical OTA testing. Research progress of the above two schemes will be conducted next.

4.4.1. Reflectarray Antennas for CATR. Complex-feeding networks to apply excitation to array elements are requirements which must be satisfied during the designing process of PWGs. To address this problem, reflectarray antennas are proposed to generate uniform plane wave. The far-field radiation pattern can be tested directly through adopting several reflectarray antennas in a closed environment to imitate the open range.

A quick method of plane wave synthesis was proposed by Wu et al. avoiding tedious calculations through embedding fast Fourier transform and fast inverse Fourier transform into Intersection Approach [77]. A model of reflectarray for calculating near field was proposed by Prado et al. to improve the performance of QZ [78]. Theories of CATR based on reflectarray were proposed by Granet et al. which was validated through a design of square reflectarray realizing a QZ bigger than 45% of the reflectarray size [79].

All the above research are theoretical. A practical experimental archetype was represented in [80] for the first time. The design in [78] realized a QZ with acceptable performance. However, the phase deviation obtained along the surface of the reflectarray was far too high to be applied. A compact reflectarray based on units composed of three parallel dipoles was proposed by Vaquero et al. for 5G devices in which a radiation near-field comprehensive technique employing amplitude and phase constraints was implemented [80]. A QZ of $100 \times 100 \times 150\,\text{mm}^3$ at 28 GHz was realized which satisfied the theoretical specifications.

However, the design in [80] is only suitable for single linear polarization. To address this problem, a single layer dual polarization reflectarray antenna was proposed by Vaquero et al. for OTA testing of 5G new radio devices in CATR system [81]. The plane wave generated by this reflectarray performed similar performance in the whole frequency band which could be applied as the low-cost testing probe in CATR system. A performance comparison of the probes above is shown in Table 9.

4.4.2. Complex-Feeding PWG. Similar to CATR, PWG also possesses the ability to directly test the far-field performance of DUT in scenes with limited space and the testing configuration is shown in Figure 8. However, the size of much smaller and the distance to the DUT are much shorter of PWG compared to CATR with equivalent testing capability especially at low frequencies. Besides, electronic phase steering realized through large PWGs costs less time compared to the mechanical steering of DUT.

Systematic research on PWG was conducted by Bucci et al. which provided references for PWG designing parameters including size, shape, and number of radiation units [82]. In addition, unified indicators for evaluating performance of PWG were also provided. A method of plane wave synthesis through antenna array was proposed by Sun et al. for OTA testing of 5G BSs which adopted genetic algorithm to optimize the amplitude and the phase of each element generating plane wave in near field [83].

Table 9: A comparison between the proposed probes in [80, 81].

No.	Aperture size (mm)	Number of layers	Amplitude ripple (dB)	Phase ripple (°)
79	188.76×188.76	single	1	10
80	190.8×190.8	single	±0.5	±5

Designs of PWG in early days mainly focused on narrowband and single polarization. However, concepts of dual-polarized PWGs with excellent performance at 5G NR FR1 were proposed. A dual-polarized PWG with broad band (0.6-6 GHz) was designed by Scattone et al. for the first time [84] which represented excellent performance. Besides, feasibility of testing antennas with low gain through PWG was validated by Scattone et al. [85], and the results were compared to the referenced values obtained in spherical near-field system taking the first step in obtaining the measurement accuracy of PWG systems.

Further, a 16×16 PWG was designed by Zhang et al. for OTA testing of 5G sub-6 GHz BSs which performed great performance including high robustness, simplicity, and low cost [86]. Several measures were employed in this design to solve the problems traditional PWG designing was facing. Firstly, a novel conical amplitude-only excitation was adopted realizing deduction in complexity of feeding network which allocated same phase excitation to each element. Besides, quaternion subarrays were employed realizing deduction in number of channel models in amplitude-phase control network which decreased the complexity of feeding network further. The measures taken above addressed the problems traditional PWG designing was facing for a long time and provided guidance for after research.

The research results above are mainly focused on sub-6 GHz, and the PWGs applied in higher frequency, namely, millimeter wave, are under common research. A PWG working at 28 GHz was designed by Xie et al. which was composed by 21×21 half-wave dipoles. Catteau et al. proposed a PWG working at FR2 frequency band for 5G NR devices which focused on analyzing the realizability of QZ. The differences between the above two PWGs are the research in [87] focused on the determination of excitation vector and the research in [88] focused on the realizability of QZ which took limitations of array elements into consideration. A comparison between the above two designs is shown in Table 10.

However, several reflectarrays or PWGs should be put around the DUT to imitate various channel models [89] which increases the testing cost conversely which contraries to the original intention. Mechanically moving the PWG around the DUT can address the above problem [90] resulting in significant increasing of time simultaneously. To overcome the above problems, the concept of a mixed chamber was proposed [91]. However, the proposals above ignored the problems occurring in practical implementation including mutual

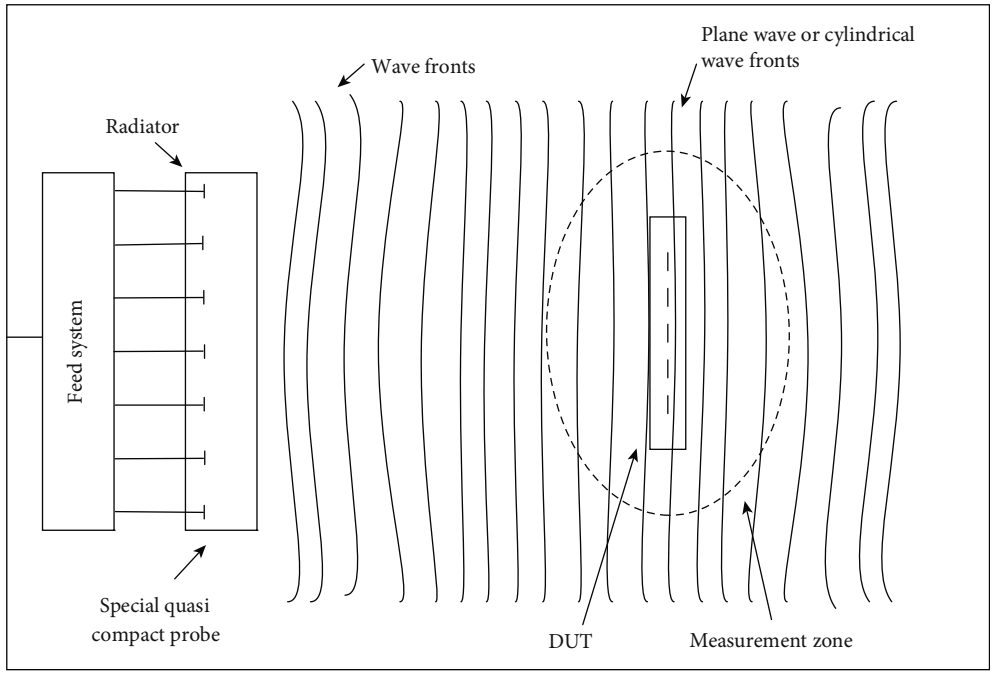

Figure 8: Measurement layout [83] of PWG for BS OTA testing.

Table 10: A comparison between the PWGs proposed in [86, 87].

No.	Operating frequency	Size (mm × mm)	AR (dB)	PR (°)	Size of QZ (mm^3)
85	FR1	1700 × 1700	1.25	1.5	900 × 900 × 2100
86	FR2	214.29 × 214.29	1	10	214.29 × 214.29 × 75

AR refers to amplitude ripple, and PR refers to phase ripple.

coupling effect between antennas, and only performance at single frequency was validated, and the robustness of the optimal solution of excitation was ignored. Regarding the above issues, Iupikov et al. proposed a designing method of element in PWG and a prototype of the mixed chamber was achieved and some testing results were shown [57]. This kind of novel fixed chambers represent excellent performance.

4.5. Alternative of Traditional Probes-Robotic Arms. The measurement efficiency of the traditional anechoic chamber-based antenna measurement is highly improved due to the introduction of multiple probes, while the employment of high-precision turntables greatly increases testing costs. The combination of artificial intelligence and antenna testing has performed outstanding advantages in recent years. Replacing the probes with a robotic arm will reduce the impact of interprobe interference on the measurement results, providing flexibility and high positioning accuracy. Robotic arm-based measurement achieves the multifunction integration of planar near-field, spherical near-field, and cylindrical near-field performing advantages including compact testing range, low cost, high accuracy, and high flexibility which effectively alleviates the shortage of testing resources and shows reference significance for technological improvement in the field of antenna measurement.

Novotny et al. [92] evaluated the performance of a robot controlled near-field measurement system [93] for measuring antennas and components from 50 GHz to 500 GHz developed by The Antenna Metrology Laboratory at the National Institute of Standards and Technology. This system is consisted of a precision industrial six-axis robot, six-axis parallel kinematic hexapod, and high-precision rotation stage. However, this system is only suitable for near-field measurements and does not support the operation of RF probes to contact integrated antennas. Boehm et al. [94] proposed a 60-330 GHz antenna measurement system consisting of a detection station, a vector network analyzer, and a six-axis industrial robotic arm which provides support not only for measurement of waveguide fed antennas but also measurement of integrated antennas.

Lebrón et al. [95] described a system called an RF scanner based on a 6-axis robotic arm for characterizing active phased array antennas which can fully automate the characterization of active phased array antennas operating at 1-18 GHz. The upper limit of the antenna frequency that can be characterized will be increased to 60 GHz if the network vector analyzer in the system can be upgraded. van Rensburg et al. [96] proposed a near-field antenna measurement system based on a robot, which consists of a 6-axis robotic arm and a 7-axis rotary locator enabling collection on a non-standard measurement plane.

Table 11: A comparison between the three OTA testing methods discussed in this paper.

Methods	Advantages	Disadvantages	Challenges	Applicability
RCM	(1) Simplicity (2) Low cost (3) High space utilization	(1) Large restriction (2) Many specific scenarios cannot be tested (3) Lack of controllable angle characteristics	Measurement on parameters related to angles	(1) Suitable for angle independent parameter testing of large devices (2) Not an international standard method for MIMO OTA testing
RTS	(1) Low cost (2) High testing efficiency	(1) Intuitive testing results (2) Not supporting beamforming antenna system (3) Limited scalability	Enhance the scalability	Adopted as standard method by 3GPP for in 5G FR1 frequency band, but with a second priority
MPAC	(1) High testing efficiency (2) Clear communication channel model (3) Clear and controllable channel angle and power characteristics	(1) High construction cost (2) Complex system calibration and operation	(1) Balancing testing costs and measurement efficiency (2) OTA testing of ultramassive antenna systems	Adopted by 3GPP as the preferred testing method for MIMO OTA

The Beijing Institute of Radio Metrology and Measurement built a planar near-field measurement system employing robots [97], and the robotic arm moves along a planar near-field scanning trajectory with a scanning plane range of 1.6 m × 1.6 m and a repeat positioning accuracy of 0.05 mm. This system can be adopted in performance measurement of antennas operating at 26.5-40 GHz. Meng et al. [98] proposed a robotic measurement system employing a robotic arm with a repeatability of 0.01 m to improve the imperfect measurement function of traditional antenna measurement systems which can be adopted to characterize antennas operating at 6-110 GHz. Parini and Gregson [99] described the simulation of a novel robotic arm-based near/far field antenna measurement system which can reconstruct the phase of measured AUT without the need of a phase reference cable and can be adopted to characterize antennas in the 100 GHz range.

4.6. Anechoic Chamber-Based Antenna Measurement in Time Domain. Antenna measurement is traditionally carried out in frequency domain (FD), and the above content is all about antenna measurement in FD. But measurement accuracy is highly depended on the physical size of the environment. As the frequency decreases, multipath reflections of waves from walls, ceilings, floors, and walkways can interfere with direct signals, seriously reducing measurement accuracy. The time-gating method (TGM) was first proposed in 1973 for measurement of antenna radiation pattern [100]. TGM is performed in time domain (TD) and can effectively eliminate multipath interference. The core idea of this method is to separate direct signals from reflected signals through using time-domain representation.

Due to the limited performance improvement of TGM for low-frequency narrowband antenna testing, Tian et al. [101] proposed a bandwidth expansion method for FD measurement systems, which achieved TGM with fast frequency sweep function and measurement of low-frequency antennas. Blech et al. [102] proposed a TD spherical near-field antenna measurement system with an operating frequency range of 1.5-8 GHz which can gate error signal components generated by multipath propagation in nonideal anechoic chambers. The system adopts switch continuous wave HW gating technology [103] which applies relatively narrowband TD gating to near-field measurements.

Piasecki and Strycharz [104] proposed a method of adopting TD technology to measure omnidirectional antenna radiation patterns without the use of anechoic chambers confirming the possibility of testing antenna radiation patterns without using anechoic chambers. González-Blanco and Sierra-Castañer [105] compared two time filtering methods for eliminating antenna measurement echoes including FFT and matrix pencil in a planar near field. However, this method presents a significant drawback of requiring multiple frequency measurements. Dadić et al. [106] proposed the real discrete Fourier transform as a time-gated method for removing reflections in antenna measurement which avoided all complex operations.

Tatomirescu [107] analyzed a low-cost measurement device for the radiation pattern of UHF band antennas but lacked experimental verification of different types of antennas with different levels of clutter illumination. Maruyama et al. [108] proposed a 28 GHz far-field estimation system which does not require reference signal input to the tested antenna and measured the near field of the antenna system in the time domain.

5. Comparison and Challenges

5.1. A Comparison between Three Methods. We have discussed the latest progress of the three testing methods above. A comparison of advantages and disadvantages and so on between these three methods is given in Table 11.

5.2. Challenges and Future Direction. OTA testing has become a mandatory requirement for terminal performance evaluation for the first time due to the new characteristics of 5G millimeter wave communication with the freezing of the 3GPP R17 standard and the gradual commercialization of millimeter wave frequencies. Each aforementioned single OTA testing method will be the ultimate solution for comprehensively and accurately characterizing 5G millimeter wave devices due to the desire for performance evaluation throughout the entire product development process and the varying testing requirements at each stage.

The optimal choice of OTA testing method is based on a balance between different performance indicators under evaluated, measurement accuracy, cost-effectiveness, complexity of testing environment, and ease of repeatability in controlled environment. Simultaneously, further requirements have been put forward for the ability of OTA testing methods due to the introduction of new testing requirements including ultramassive terminals and small testing chambers. Millimeter wave OTA testing methods are also evolving, improving, and perfecting to meet the growing needs of the industry.

In addition to being fully utilized in 5G, millimeter wave technology will also play an important role in 6G. Therefore, the testing methods of 5G millimeter wave equipment will also affect future 6G equipment. Developing testing methods which possess higher efficiency, lower cost, and lower complexity testing systems will have significant implications for 6G.

6. Contributions

In this article, we summarize the latest progress in OTA testing methods including reverberation chamber-based method, radiated two-stage method, and MPAC method in recent years based on the latest technological development requirements of OTA testing. A detailed summary of testing parameters including the application scenarios, advantages, and disadvantages of the three methods is provided in this paper which is more detailed and comprehensive compared to other review articles. This paper focuses on mastering and elaborating on the latest progress of MPAC methods among the three OTA testing methods. The specific contributions of this paper are summarized as the following aspects.

(1) We summarize the newest progress of the reverberation chamber-based method. In this section, this paper summarizes the latest progress of reverberation chamber testing methods and provides a detailed classification overview of this testing method based on different testing parameters

(2) As an OTA testing method specified by the 3GPP standard, this article summarizes the latest development of the radiated two-step method

(3) This paper elaborates on the latest progress of MPAC methods and provides corresponding future development directions. In this section, the latest progress in MPAC testing methods is summarized based on different configurations including 2-D MPAC, 3-D MPAC, and 3-D sectored MPAC. In each subsection, detailed comparisons are made for the specific parameters, application scenarios, probe configurations, and other parameters between different methods. Besides, detailed explanations are provided on the configuration and selection of probes to reduce testing costs. Finally, the future development direction of MPAC method is pointed out

In summary, this paper provides a detailed overview of the latest developments on three OTA testing methods and introduces the latest developments in the 3GPP standard. In addition, the potential challenges and future development directions of 5G MIMO OTA testing are elaborated.

7. Conclusion

In this paper, we discuss the three main methods of OTA testing including RC-based method, RTS method, and MPAC-based method with MPAC-based method highlighted. Several aspects of the MPAC-based method are discussed including probe configurations, probe design, and probe selection algorithms, and recent literature work is summarized. The PFS technique has been extensively validated in MPAC systems while the design of PWGs still faces significant challenges in the future. A detailed comparison between the above three OTA testing methods is made. Probe design is also an important development direction for OTA testing in the future. For the purpose of further reducing the measurement cost and required space of OTA testing, the development of compact anechoic chambers will be further promoted in the future taking an anechoic chamber with a volume of $1\text{m} \times 1\text{m} \times 1\text{m}$ as an example.

Conflicts of Interest

The authors declare that they have no conflicts of interest.

Acknowledgments

This work was supported by the National Key Research and Development Program of China (No. 2022YFF0604300) and the National Natural Science Foundation of China (No. 61821001).

References

[1] 3GPP Technical Report 37.977 v14.5.0, *Verification of Radiated Multi-antenna Reception Performance of User Equipment (UE)*, 3GPP, 2017.

[2] W. Fan, G. F. Pedersen, P. Kyösti, A. Hekkala, T. Jämsä, and M. Gustafsson, "Recent advances on OTA testing for 5G antenna systems in multi-probe anechoic chamber setups," in *2017 Sixth Asia-Pacific Conference on Antennas and Propagation (APCAP)*, pp. 1–3, Xi'an, China, October 2017.

[3] W. Fan, I. Carton, P. Kyosti et al., "A step toward 5G in 2020: low-cost OTA performance evaluation of massive MIMO base stations," *IEEE Antennas and Propagation Magazine*, vol. 59, no. 1, pp. 38–47, 2017.

[4] P. Kyösti, T. Jämsä, and J. P. Nuutinen, "Channel modelling for multiprobe over-the-air MIMO testing," *International Journal of Antennas and Propagation*, vol. 2012, Article ID 615954, 11 pages, 2012.

[5] P. Shen, Y. Qi, W. Yu, F. Li, and J. Fan, "Fast and accurate TIS testing method for wireless user equipment with RSS reporting," *IEEE Transactions on Electromagnetic Compatibility*, vol. 58, no. 3, pp. 887–895, 2016.

[6] Z. Liu, Y. Qi, F. Li, W. Yu, J. Fan, and J. Chen, "Fast band-sweep total isotropic sensitivity measurement," *IEEE Transactions on Electromagnetic Compatibility*, vol. 58, no. 4, pp. 1244–1251, 2016.

[7] X. Yang, H. Sun, F. Wang, S. Qiao, and Y. Ren, "Standardization progress and challenges for 5G MIMO OTA performance testing," in *2022 IEEE 5th International Conference on Electronic Information and Communication Technology (ICEICT)*, pp. 505–507, Hefei, China, August 2022.

[8] H. Kong, Y. Jing, Z. Wen, and L. Cao, "Mid-field OTA RF test method: new developments and performance comparison with the compact antenna test range (CATR)," in *2020 14th European Conference on Antennas and Propagation (EuCAP)*, pp. 1–5, Copenhagen, Denmark, March 2020.

[9] Y. Liu, X. Sun, and Y. Zhou, "Challenges and applicability of OTA measurement for 5G millimeter wave mobile device," in *2021 Cross Strait Radio Science and Wireless Technology Conference (CSRSWTC)*, pp. 16–18, Shenzhen, China, October 2021.

[10] X. Yi, S. Zhang, B. Zhou, Y. Deng, and S. Zhu, "MIMO OTA testing for 5G user equipment: standardization progress and challenges," in *2023 17th European Conference on Antennas and Propagation (EuCAP)*, pp. 1–3, Florence, Italy, March 2023.

[11] Y. Jing, T. Hertel, H. Kong, P. Shen, and Y. Liu, "Recent developments in radiated two-stage MIMO OTA test method," in *2020 14th European Conference on Antennas and Propagation (EuCAP)*, pp. 1–5, Copenhagen, Denmark, March 2020.

[12] F. Yu, N. Ma, X. Yang, and J. Chen, "Flexible sectorized MPAC configuration for 5G OTA testing," in *2020 IEEE 20th International Conference on Communication Technology (ICCT)*, pp. 476–481, Nanning, China, 2020.

[13] M. L. Bäckström, O. Lundén, and P. S. Kildal, "Reverberation chambers for EMC susceptibility and emission analyses," *Review of Radio Science*, pp. 429–452, Wiley-Interscience, 1999.

[14] A. Khaleghi, "Time-domain measurement of antenna efficiency in reverberation chamber," *IEEE Transactions on Antennas and Propagation*, vol. 57, no. 3, pp. 817–821, 2009.

[15] H. G. Krauthäuser and M. Herbrig, "Yet another antenna efficiency measurement method in reverberation chambers," in *2010 IEEE International Symposium on Electromagnetic Compatibility*, pp. 536–540, Fort Lauderdale, FL, USA, July 2010.

[16] M. Piette, "Antenna radiation efficiency measurements in a reverberation chamber," in *2004 Asia-Pacific Radio Science Conference, 2004. Proceedings*, pp. 19–22, Qingdao, China, August 2004.

[17] P.-S. Kildal and K. Rosengren, "Correlation and capacity of MIMO systems and mutual coupling, radiation efficiency, and diversity gain of their antennas: simulations and measurements in a reverberation chamber," *IEEE Communications Magazine*, vol. 42, no. 12, pp. 104–112, 2004.

[18] "IEC61000-4-21: EMC, Part 4: Testing and Measurement Techniques; Section 21: Reverberation Chamber Test Methods," in *ES-AENOR*, International Electrotechnical Commission, Committee Draft, Geneva, 2001.

[19] A. A. H. Azremi, H. G. Shiraz, and P. S. Hall, "Reverberation chamber for efficiency measurement of small antennas," in *2005 1st International Conference on Computers, Communications, & Signal Processing with Special Track on Biomedical Engineering*, pp. 25–29, Kuala Lumpur, Malaysia, November 2005.

[20] H. A. Wheeler, "The radiansphere around a small antenna," *Proceedings of the IRE*, vol. 47, no. 8, pp. 1325–1331, 1959.

[21] A. A. H. Azremi, H. G. Shiraz, and P. S. Hall, "Small antenna efficiency by the reverberation chamber and the Wheeler Cap methods," in *2005 13th IEEE International Conference on Networks Jointly held with the 2005 IEEE 7th Malaysia International Conf on Communic*, pp. 12–16, Kuala Lumpur, Malaysia, November 2005.

[22] C. S. Lee, A. Duffy, and C. Lee, "Antenna efficiency measurements in a reverberation chamber without the need for a reference antenna," *IEEE Antennas and Wireless Propagation Letters*, vol. 7, pp. 448–450, 2008.

[23] C. L. Holloway, H. A. Shah, R. J. Pirkl, W. F. Young, D. A. Hill, and J. Ladbury, "Reverberation chamber techniques for determining the radiation and total efficiency of antennas," *IEEE Transactions on Antennas and Propagation*, vol. 60, no. 4, pp. 1758–1770, 2012.

[24] Q. Xu, Y. Huang, X. Zhu, L. Xing, Z. Tian, and C. Song, "A modified two-antenna method to measure the radiation efficiency of antennas in a reverberation chamber," *IEEE Antennas and Wireless Propagation Letters*, vol. 15, pp. 336–339, 2016.

[25] V. Fiumara, A. Fusco, V. Matta, and I. M. Pinto, "Free-space antenna field/pattern retrieval in reverberation environments," *IEEE Antennas and Wireless Propagation Letters*, vol. 4, pp. 329–332, 2005.

[26] C. Lemoine, E. Amador, P. Besnier, J.-M. Floc'h, and A. Laisne, "Antenna directivity measurement in reverberation chamber from Rician K-factor estimation," *IEEE Transactions on Antennas and Propagation*, vol. 61, no. 10, pp. 5307–5310, 2013.

[27] V. Fiumara, A. Fusco, G. Iadarola, V. Matta, and I. M. Pinto, "Free-space antenna pattern retrieval in nonideal reverberation chambers," *IEEE Transactions on Electromagnetic Compatibility*, vol. 58, no. 3, pp. 673–677, 2016.

[28] M. Á. García-Fernández, D. Carsenat, and C. Decroze, "Antenna radiation pattern measurements in reverberation chamber using plane wave decomposition," *IEEE Transactions on Antennas and Propagation*, vol. 61, no. 10, pp. 5000–5007, 2013.

[29] M. Á. García-Fernández, D. Carsenat, and C. Decroze, "Antenna gain and radiation pattern measurements in reverberation chamber using Doppler effect," *IEEE Transactions on Antennas and Propagation*, vol. 62, no. 10, pp. 5389–5394, 2014.

[30] Q. Xu, Y. Huang, L. Xing et al., "3-D antenna radiation pattern reconstruction in a reverberation chamber using spherical wave decomposition," *IEEE Transactions on Antennas and Propagation*, vol. 65, no. 4, pp. 1728–1739, 2017.

[31] J. Zheng, X. Chen, X. Liu, M. Zhang, B. Liu, and Y. Huang, "An improved method for reconstructing antenna radiation pattern in a loaded reverberation chamber," *IEEE Transactions on Instrumentation and Measurement*, vol. 71, pp. 1–12, 2022.

[32] A. K. Puls, J. M. Ladbury, and W. F. Young, "Antenna radiation pattern measurements using a reverberation chamber," in *2018 AMTA Proceedings*, pp. 1–6, Williamsburg, VA, USA, November 2018.

[33] 3GPP TR38.827, *Study on Radiated Metrics and Test Methodology for the Verification of Multi-antenna Reception Performance of NR User Equipment (Release 17)*, 3GPP (3rd Generation Partnership Project), 2021.

[34] W. Yu, Y. Qi, K. Liu, Y. Xu, and J. Fan, "Radiated two-stage method for LTE MIMO user equipment performance evaluation," *IEEE Transactions on Electromagnetic Compatibility*, vol. 56, no. 6, pp. 1691–1696, 2014.

[35] Y. Jing, M. Rumney, H. Kong, and Z. Wen, "Analysis of applicability of radiated two-stage test method to 5G radiated performance measurement," in *12th European Conference on Antennas and Propagation (EuCAP 2018)*, pp. 1–5, London, UK, April 2018.

[36] P. Shen, Y. Qi, W. Yu, and J. Fan, "UE reporting uncertainty analysis in radiated two-stage MIMO measurements," *IEEE Transactions on Antennas and Propagation*, vol. 69, no. 12, pp. 8808–8815, 2021.

[37] W. Wang, R. Wang, H. Gao, and Y. Wu, "Implementation and analysis of 3D channel emulation method in multiprobe anechoic chamber setups," *IEEE Access*, vol. 7, pp. 108571–108580, 2019.

[38] P. Kyösti, J.-P. Nuutinen, J. Kolu, and M. Falck, "Channel modelling for radiated testing of MlMO capable terminals," in *ICT Mobile Summit Conference*, pp. 1–8, Santander, Spain, June 2009.

[39] T. Imai, Y. Okano, K. Koshiro, K. Saito, and S. Miura, "Theoretical analysis of adequate number of probe antennas in spatial channel emulator for MIMO performance evaluation of mobile terminals," in *Proceedings of the Fourth European Conference on Antennas and Propagation*, pp. 1–5, Barcelona, Spain, April 2010.

[40] T. Laitinen, P. Kyösti, J.-P. Nuutinen, and P. Vainikainen, "On the number of OTA antenna elements for plane-wave synthesis in a MIMO-OTA test system involving a circular antenna array," in *Proceedings of the Fourth European Conference on Antennas and Propagation*, pp. 1–5, Barcelona, Spain, April 2010.

[41] W. Fan, I. Szini, J. Ø. Nielsen, and G. F. Pedersen, "Channel spatial correlation reconstruction in flexible multiprobe setups," *IEEE Antennas and Wireless Propagation Letters*, vol. 12, pp. 1724–1727, 2013.

[42] R. Fan, W. Sun, and S. Shi, "Probe selection algorithm for massive MIMO base station OTA testing," in *2019 IEEE Asia-Pacific Microwave Conference (APMC)*, pp. 1349–1351, Singapore, 2019.

[43] H. Wang, C. Wang, W. Wang, G. Zhang, Y. Wu, and Y. Liu, "Flexible OTA probe setups for massive MIMO base station testing," in *2018 Asia-Pacific Microwave Conference (APMC)*, pp. 908–910, Kyoto, Japan, 2018.

[44] X. Yang, H. Sun, Y. Guo, S. Qiao, and Z. Wang, "A novel probe selection algorithm based on standard FR1 MIMO OTA testing solutions," in *2022 IEEE 95th Vehicular Technology Conference: (VTC2022-Spring)*, pp. 1–5, Helsinki, Finland, June 2022.

[45] H. Sun, X. Yang, Y. Zhu, and Z. Wang, "An efficient probe selection method for 5G base station OTA testing with MPAC setup," in *2022 IEEE 96th Vehicular Technology Conference (VTC2022-Fall)*, pp. 1–5, London, United Kingdom, 2022.

[46] P. Kyösti and A. Khatun, "Probe configurations for 3D MIMO over-the-air testing," in *2013 7th European Conference on Antennas and Propagation (EuCAP)*, pp. 1421–1425, Gothenburg, Sweden, April 2013.

[47] W. Fan, F. Sun, J. Ø. Nielsen et al., "Probe selection in multiprobe OTA setups," *IEEE Transactions on Antennas and Propagation*, vol. 62, no. 4, pp. 2109–2120, 2014.

[48] W. Fan, X. C. B. de Lisbona, F. Sun, J. O. Nielsen, M. B. Knudsen, and G. F. Pedersen, "Emulating spatial characteristics of MIMO channels for OTA testing," *IEEE Transactions on Antennas and Propagation*, vol. 61, no. 8, pp. 4306–4314, 2013.

[49] H. Gao, W. Wang, Y. Wu, and Y. Liu, "3D flexible multiprobe setups for MIMO OTA testing," in *2017 IEEE 5th International Symposium on Electromagnetic Compatibility (EMC-Beijing)*, pp. 1–4, Beijing, China, October 2017.

[50] W. Fan, P. Kyosti, S. Fan et al., "3D channel model emulation in a MIMO OTA setup," in *2013 IEEE 78th Vehicular Technology Conference (VTC Fall)*, pp. 1–5, Las Vegas, NV, USA, September 2013.

[51] Y. Yuan, W. Wang, Y. Liu, Y. Wu, and K. Liu, "Impact of probe ring location on test area performance in 3D MIMO OTA setup," in *2016 11th International Symposium on Antennas, Propagation and EM Theory (ISAPE)*, pp. 858–861, Guilin, China, October 2016.

[52] W. Weimin, L. Muyuan, L. Yuan'an, W. Yongle, and L. Shulan, "Novel physical probe configurations in a multiprobe based 3D MIMO OTA setup," *The Journal of China Universities of Posts and Telecommunications*, vol. 24, no. 1, pp. 60–66, 2017.

[53] Z. Wang, Z. Jiang, Z.-C. Hao, and W. Hong, "A novel probe selection method for MIMO OTA performance testing," *IEEE Antennas and Wireless Propagation Letters*, vol. 19, no. 12, pp. 2359–2362, 2020.

[54] X. Yang, P. Zhang, J. Chen, N. Ma, and B. Liu, "Probe subset selection in 3D multiprobe OTA setup," in *2018 IEEE 29th Annual International Symposium on Personal, Indoor and Mobile Radio Communications (PIMRC)*, pp. 1–6, Bologna, Italy, 2018.

[55] Y. Guo, Y. Zhang, X. Yang, J. Zhang, and Z. Wang, "5G multifunctional MPAC test solution based on switch matrix and probe selection," in *2022 IEEE 96th Vehicular Technology Conference (VTC2022-Fall)*, pp. 1–5, London, United Kingdom, 2022.

[56] J. Wang, N. Ma, and B. Liu, "A novel probe selection method for MIMO OTA test," in *2022 IEEE Wireless Communications and Networking Conference (WCNC)*, pp. 1557–1562, Austin, TX, USA, 2022.

[57] O. A. Iupikov, P. S. Krasov, A. A. Glazunov, R. Maaskant, J. Friden, and M. V. Ivashina, "Hybrid OTA chamber for multidirectional testing of wireless devices: plane wave spectrum generator design and experimental demonstration," *IEEE Transactions on Antennas and Propagation*, vol. 70, no. 11, pp. 10974–10987, 2022.

[58] P. Kyösti, L. Hentilä, W. Fan, J. Lehtomäki, and M. Latva-Aho, "On radiated performance evaluation of massive MIMO devices in multiprobe anechoic chamber OTA setups," *IEEE Transactions on Antennas and Propagation*, vol. 66, no. 10, pp. 5485–5497, 2018.

[59] Y. Li, H. Sun, X. Chen, L. Xin, and X. Zhang, "Probe selection and power weighting in multiprobe OTA testing: a neural network-based approach," *International Journal of Antennas and Propagation*, vol. 2019, Article ID 1392129, 8 pages, 2019.

[60] X. Zhang, S. Qiao, M. Peng, and Y. Li, "Probe selection for over-the-air test in 5G base stations with massive multiple-input multiple-output," *China Communications*, vol. 16, no. 7, pp. 1–12, 2019.

[61] H. Wang, W. Wang, Y. Wu, B. Tang, W. Zhang, and Y. Liu, "Probe selection for 5G massive MIMO base station over-the-air testing," *IEEE Antennas and Wireless Propagation Letters*, vol. 19, no. 11, pp. 1998–2002, 2020.

[62] Q. Zhang, X. Shi, S. Gao et al., "Highly integrated transmitting and receiving phased array with multi-channels and high efficiency in K/Ka-band SatCom application," *International Journal of RF and Microwave Computer-Aided Engineering*, vol. 31, no. 10, 2021.

[63] D. C. Dinis, N. B. Carvalho, A. S. R. Oliveira, and J. Vieira, "Over the air characterization for 5G massive MIMO array transmitters," in *2017 IEEE MTT-S International Microwave Symposium (IMS)*, pp. 1441–1444, Honolulu, HI, USA, 2017.

[64] N. B. Carvalho, K. A. Remley, D. Schreurs, and K. G. Card, "Multisine signals for wireless system test and design [application notes]," *IEEE Microwave Magazine*, vol. 9, no. 3, pp. 122–138, 2008.

[65] M. Jordão, D. Belo, and N. B. Carvalho, "Active antenna array characterization for massive MIMO 5G scenarios," in *2018 91st ARFTG Microwave Measurement Conference (ARFTG)*, pp. 1–4, Philadelphia, PA, USA, 2018.

[66] M. Jordão, D. Belo, R. F. S. Caldeirinha, A. S. R. Oliveira, and N. B. de Carvalho, "Over-the-air calibration of active antenna arrays using multisine," *IEEE Transactions on Microwave Theory and Techniques*, vol. 69, no. 1, pp. 431–442, 2021.

[67] X. Zhang, Z. Wang, C. Pan, X. Ba, and Y. Wang, "Dual-polarized inverted quad-ridged flared horn antenna with one-decade bandwidth for OTA testing," *IEEE Antennas and Wireless Propagation Letters*, vol. 21, no. 6, pp. 1233–1237, 2022.

[68] Y. Qi, G. Yang, L. Liu et al., "5G over-the-air measurement challenges: overview," *IEEE Transactions on Electromagnetic Compatibility*, vol. 59, no. 6, pp. 1661–1670, 2017.

[69] F. Lin, J. Fan, Y. Qi, and Y. Jiao, "Study of cross polarization of tapered slot antenna for EMC measurements," in *2013 IEEE International Symposium on Electromagnetic Compatibility*, pp. 12–16, Denver, CO, USA, 2013.

[70] F. Lin, Y. Qi, J. Fan, and Y.-C. Jiao, "0.7–20-GHz dual-polarized bilateral tapered slot antenna for EMC measurements," *IEEE Transactions on Electromagnetic Compatibility*, vol. 56, no. 6, pp. 1271–1275, 2014.

[71] K. Ebnabbasi, S. Sczyslo, and M. Mohebbi, "UWB performance of coplanar tapered slot antennas," *IEEE Antennas and Wireless Propagation Letters*, vol. 12, pp. 749–752, 2013.

[72] H. Oraizi and S. Jam, "Optimum design of tapered slot antenna profile," *IEEE Transactions on Antennas and Propagation*, vol. 51, no. 8, pp. 1987–1995, 2003.

[73] M. Sonkki, D. Sánchez-Escuderos, V. Hovinen, E. T. Salonen, and M. Ferrando-Bataller, "Wideband dual-polarized cross-shaped Vivaldi antenna," *IEEE Transactions on Antennas and Propagation*, vol. 63, no. 6, pp. 2813–2819, 2015.

[74] J. Wu, Y. Qi, W. Yu, L. Liu, and F. Li, "An absorber-integrated taper slot antenna," *IEEE Transactions on Electromagnetic Compatibility*, vol. 59, no. 6, pp. 1741–1747, 2017.

[75] Z. Qiao, Z. Wang, T.-H. Loh, S. Gao, and J. Miao, "A compact minimally invasive antenna for OTA testing," *IEEE Antennas and Wireless Propagation Letters*, vol. 18, no. 7, pp. 1381–1385, 2019.

[76] A. Murugesan, K. T. Selvan, A. Iyer, K. V. Srivastava, and A. Alphones, "A review of metasurface-assisted RCS reduction techniques," *Progress In Electromagnetics Research B*, vol. 94, pp. 75–103, 2021.

[77] Y. Wu, J. Wu, and Z. Li, "Plane wave synthesis using near field wave spectrum transform embedded into intersection approach," in *2018 International Conference on Microwave and Millimeter Wave Technology (ICMMT)*, pp. 1–3, Chengdu, China, 2018.

[78] D. R. Prado, A. F. Vaquero, M. Arrebola, M. R. Pino, and F. Las-Heras, "General near field synthesis of reflectarray antennas for their use as probes in CATR," *Progress In Electromagnetics Research*, vol. 160, pp. 9–17, 2017.

[79] C. Granet, M. Zhou, S. B. Sørensen, K. W. Smart, J. S. Kot, and J. Ness, "Reflectarray compact antenna test range concept," in *2019 13th European Conference on Antennas and Propagation (EuCAP)*, pp. 1–5, Krakow, Poland, 2019.

[80] Á. F. Vaquero, M. Arrebola, M. R. Pino, R. Florencio, and J. A. Encinar, "Demonstration of a reflectarray with near-field amplitude and phase constraints as compact antenna test range probe for 5G new radio devices," *IEEE Transactions on Antennas and Propagation*, vol. 69, no. 5, pp. 2715–2726, 2021.

[81] Á. F. Vaquero, R. Florencio, M. R. Pino, and M. Arrebola, "Dual-polarized near-field plane wave generator using an offset-optics reflectarray Mm-wave band," *IEEE Transactions on Antennas and Propagation*, vol. 70, no. 12, pp. 12370–12375, 2022.

[82] O. M. Bucci, M. D. Migliore, G. Panariello, and D. Pinchera, "Plane-wave generators: design guidelines, achievable performances and effective synthesis," *IEEE Transactions on Antennas and Propagation*, vol. 61, no. 4, pp. 2005–2018, 2013.

[83] S. Sun, N. Wang, X. Ma, S. Zhu, and R. Wang, "Design of plane wave generator in compact range for 5G OTA testing," in *2019 Photonics & Electromagnetics Research Symposium-Fall (PIERS-Fall)*, pp. 1011–1014, Xiamen, China, 2019.

[84] F. Scattone, D. Sekuljica, A. Giacomini et al., "Design of dual polarised wide band plane wave generator for direct far-field testing," in *2019 13th European Conference on Antennas and Propagation (EuCAP)*, pp. 1–4, Krakow, Poland, 2019.

[85] F. Scattone, D. Sekuljica, A. Giacomini et al., "Comparative testing of devices in a spherical near field system and plane wave generator," in *2019 Antenna Measurement Techniques Association Symposium (AMTA)*, pp. 1–3, San Diego, CA, USA, 2019.

[86] Y. Zhang, Z. Wang, X. Sun, Z. Qiao, W. Fan, and J. Miao, "Design and implementation of a wideband dual-polarized plane wave generator with tapered feeding nonuniform array," *IEEE Antennas and Wireless Propagation Letters*, vol. 19, no. 11, pp. 1988–1992, 2020.

[87] R. Xie, X. Wang, R. Wang et al., "Synthesis of plane wave applied to 5G communication antenna measurement," in *2017 Progress In Electromagnetics Research Symposium-Spring (PIERS)*, pp. 195–198, St. Petersburg, Russia, 2017.

[88] S. Catteau, M. Ivashina, and R. Rehammar, "Design and simulation of a 28 GHz plane wave generator for NR measurements," in *2020 14th European Conference on Antennas and Propagation (EuCAP)*, pp. 1–4, Copenhagen, Denmark, 2020.

[89] C. Rowell, B. Derat, and A. Cardalda-Garcia, "Multiple CATR reflector system for 5G radio resource management measurements," in *2021 15th European Conference on Antennas and Propagation (EuCAP)*, pp. 1–5, Dusseldorf, Germany, 2021.

[90] F. Scattone, D. Sekuljica, A. Giacominil et al., "Towards testing of 5G millimeter wave devices using plane wave generators," in *2021 15th European Conference on Antennas and Propagation (EuCAP)*, pp. 1–4, Dusseldorf, Germany, March 2021.

[91] R. Maaskant, O. A. Iupikov, P. S. Krasov, R. Rehammar, A. A. Glazunov, and M. V. Ivashina, "A new hybrid chamber for generating a spectrum of oblique incident plane waves at the DUT," *IEEE Transactions on Antennas and Propagation*, vol. 69, no. 10, pp. 6806–6815, 2021.

[92] D. Novotny, J. Gordon, J. Coder, M. Francis, and J. Guerrieri, "Performance evaluation of a robotically controlled millimeter-wave near-field pattern range at the NIST," in *2013 7th European Conference on Antennas and Propagation (EuCAP)*, pp. 4086–4089, Gothenburg, Sweden, June 2013.

[93] J. Gordon, D. Novotny, J. Coder, J. Guerrieri, and B. Stillwell, "Robotically controlled mm-wave near-field pattern range," *Proceed. Antenna Measurement Techniques Assoc*, pp. 384–389, Bellview, WA, 2012.

[94] L. Boehm, F. Boegelsack, M. Hitzler, and C. Waldschmidt, "An automated millimeter-wave antenna measurement setup using a robotic arm," in *2015 IEEE International Symposium on Antennas and Propagation & USNC/URSI National Radio Science Meeting*, pp. 2109-2110, Vancouver, BC, Canada, July 2015.

[95] R. M. Lebrón, J. L. Salazar, C. Fulton, S. Duthoit, D. Schmidt, and R. Palmer, "A novel near-field robotic scanner for surface, RF and thermal characterization of millimeter-wave active phased array antenna," in *2016 IEEE International Symposium on Phased Array Systems and Technology (PAST)*, pp. 1–6, Waltham, MA, USA, October 2016.

[96] D. J. van Rensburg, B. Walkenhorst, Q. Ton, and J. Demas, "A robotic near-field antenna test system relying on non-canonical transformation techniques," in *2019 Antenna Measurement Techniques Association Symposium (AMTA)*, pp. 1–5, San Diego, CA, USA, October 2019.

[97] X. Liu, C. Huang, and Y. Cheng, "Antenna planar near-field measurement system using robotics," in *2021 13th Global Symposium on Millimeter-Waves & Terahertz (GSMM)*, pp. 1–3, Nanjing, China, May 2021.

[98] M. Meng, A. Wu, Z. Stokesberry, T. Zhao, S. Y. Lee, and N. Ghalichechian, "Robotic radiation pattern measurement system for 6–110 GHz based in both near field and far field," in *2023 IEEE International Opportunity Research Scholars Symposium (ORSS)*, pp. 11–15, Atlanta, GA, USA, April 2023.

[99] C. G. Parini and S. F. Gregson, "Simulation of a novel phase retrieval technique for multi-axis robotic arm based near-field antenna measurements," in *2023 17th European Conference on Antennas and Propagation (EuCAP)*, pp. 1–5, Florence, Italy, March 2023.

[100] G. Burrell and A. Jamieson, "Antenna radiation pattern measurement using time-to-frequency transformation (TFT) techniques," *IEEE Transactions on Antennas and Propagation*, vol. 21, no. 5, pp. 702–704, 1973.

[101] J. Tian, L. Zhang, N. Li, and W. Chen, "Time-gating method for V/UHF antenna pattern measurement inside an anechoic chamber," in *2008 International Conference on Microwave and Millimeter Wave Technology*, pp. 942–945, Nanjing, April 2008.

[102] M. D. Blech, M. M. Leibfritz, R. Hellinger et al., "Time-domain spherical near-field antenna measurement system employing a switched continuous-wave hardware gating technique," *IEEE Transactions on Instrumentation and Measurement*, vol. 59, no. 2, pp. 387–395, 2010.

[103] M. M. Leibfritz, M. D. Blech, F. M. Landstorfer, and T. F. Eibert, "A comparison of software- and hardware-gating techniques applied to near-field antenna measurements," *Advances in Radio Science*, vol. 5, pp. 43–48, 2007.

[104] P. Piasecki and J. Strycharz, "Measurement of an omnidirectional antenna pattern in an anechoic chamber and an office room with and without time domain signal processing," in *2015 Signal Processing Symposium (SPSympo)*, pp. 1–4, Debe, Poland, June 2015.

[105] P. González-Blanco and M. Sierra-Castañer, "Time filtering techniques for echo reduction in antenna measurements," in *2016 10th European Conference on Antennas and Propagation (EuCAP)*, pp. 1–3, Davos, Switzerland, April 2016.

[106] M. Dadić, R. Zentner, and Ž. Lenić, "Time-gating in antenna and microwave measurements using RDFT," in *2016 22nd International Conference on Applied Electromagnetics and Communications (ICECOM)*, pp. 1–4, Dubrovnik, Croatia, September 2016.

[107] A. Tatomirescu, "UHF band antenna radiation pattern measurements in multipath channel using time domain gating," in *2020 International Workshop on Antenna Technology (iWAT)*, pp. 1–4, Bucharest, Romania, February 2020.

[108] Y. Maruyama, K. Fujimori, H. Arai, and T. Tanaka, "Proposal of time domain near-field measurement system for 5G antenna system," in *2020 International Symposium on Antennas and Propagation (ISAP)*, pp. 259-260, Osaka, Japan, January 2021.